*Physics – Uspekhi* **43** (11) 1137 – 1145 (2000) 

*FROM THE CURRENT LITERATURE*

PACS numbers: 02.30.Px, **12.38. – t**, **13.85. – t**, **13.87. – a**

# Long-range particle correlations and wavelets

I M Dremin

DOI: 10.1070/PU2000v043n11ABEH000866

## Contents



**Abstract. The problem of long-range correlations of particles produced in high-energy collisions is discussed. Long-range correlations may involve large groups of particles, as exemplified by the ring-like and elliptic flow patterns of individual high-multiplicity events in the polar and azimuthal angle planes. To identify such structures, a wavelet-analysis technique has been proposed and applied to some central lead-lead collisions at an energy of 158 GeV per nucleon. In the present paper, previous attempts at obtaining long-range correlations are discussed and recent wavelet-analysis results for high energy nucleus-nucleus interactions are reviewed.**

## 1. Introduction

Recently, in Brookhaven National Laboratory (USA) the RHIC collider started operating, where the colliding beams of the nuclei of heavy elements interact with each other at a total energy of up to 200 GeV per nucleon in the center-of-mass system. There are some interesting (although still preliminary) first results, in particular, about the multiplicities of particles produced. It turned out, that, if recalculated per nucleon of the colliding nuclei, the multiplicity exceeds that of nucleon – nucleon collisions at the same energy in the center-of-mass system. Studying events with a multiplicity of produced charged particles of up to 10000 will soon become available. With the advent of the LHC collider in CERN (Switzerland), when the energy of colliding nuclei will increase to 14 TeV per nucleon, events with the production of up to 20000 charged particles will be available.

The problem of representation and analysis of such high multiplicity events becomes rather non-trivial. Each particle can be represented by a dot in the 3-dimensional phase space. Therefore, the distribution of these dots can be found for a single event. Different patterns formed by these dots in the phase space would correspond to different correlations and, therefore, to different dynamics. The problem of finding and deciphering these patterns becomes crucial for understanding the underlying dynamics. Really we are entering a new stage of studies of multiparticle production processes, where, apart from the traditional methods of selecting definite events with the use of triggers or displaying the plots of the simplest inclusive distributions, the exclusive characteristics of individual events with high multiplicities become important in event-by-event analysis. To classify these patterns, one should develop adequate methods for their recognition and analysis. The wavelet analysis is just such a suitable method. Nowadays, the very first attempts (discussed in this paper) to apply this method are known, and it will, surely, find wider application.

Various correlations of particles produced in high-energy collisions are known. Especially well studied are the two-particle correlations due to the decay of two-particle resonances or to the Bose – Einstein effect for identical particles. The common correlation function technique, well known, for example, in statistical physics, is well suited for the analysis of these two-particle correlations. It is more difficult to apply this technique if several particles are involved, because the correlation functions for three or more particles depend on many variables and, therefore, are difficult to handle. Nevertheless, correlations leading to the formation of clusters (or mini-jets, non-reducible to resonances) and jets (the correlated systems of many particles with common angular characteristics of their emission directions) have been studied as well, however, mostly in $e^+e^-$-collisions, where jet and subjet structures are clearly visible. Otherwise one has to apply averaging procedures to obtain knowledge of dynamical correlations from the moments of various distributions and from their behavior in different regions of the phase space (for recent reviews, see [1 – 3]). This has led to the understanding of such global features as the intermittent dynamics (first considered in Ref. [4]) and the fractal structure of phase space distributions (first considered in Ref. [5]) in these processes. It has been shown [6 – 8] that, even at the level of the lowest perturbative approximations, quantum chromodynamics (QCD) explains, at least qualitatively, this

**I M Dremin** P N Lebedev Physics Institute, Russian Academy of Sciences
Leninskiĭ prosp. 53, 117924 Moscow, Russian Federation
Tel. (7-095) 132 29 29. Fax (7-095) 135 85 33
E-mail: dremin@lpi.ru

Received 15 September 2000
*Uspekhi Fizicheskikh Nauk* **170** (11) 1235 – 1244 (2000)
Translated by I M Dremin; edited by A V Getling

structure as resulting from the intermittent emission of jets with progressively diminishing energies. Some completely new and unexpected features such as oscillating cumulant correlators of the multiplicity distributions were predicted in QCD [9, 10] and confirmed by experiment (see, e.g., the review papers [2, 3]). This demonstrated the existence of repulsive correlations, besides the attractive correlations, between groups with different numbers of particles.

However, the genuine multiparticle correlations originating from some collective effects may still be hidden in individual events. It is not clear if they can be disentangled with such averaging methods, especially if their probability is not high. These local effects could be seen in some (probably, rare) events as special patterns formed by particles produced within the available phase space. They should be separated from statistical fluctuations leading to similar patterns. It is the method of wavelet analysis that allows the recognition of patterns due to correlations at different scales and to damp down the statistical noise even if it is very large in the original sample [11 – 14]. The ability to reveal the local properties of a process is the main advantage of wavelet analysis compared to other methods, in particular, to Fourier analysis (for more detailed discussion see Ref. [14]). In its turn, this article provides a more detailed review of one of the problems briefly described in Ref. [14].

## 2. About some long-range correlations

Before delving into the applications of this method, let us consider some examples of possible correlations which one might seek. A well known example of long-range correlations is provided, e.g., by the forward-backward correlations. However, they are of a global nature, while we are more interested here in such correlations which lead to special long-correlated patterns in the available phase space. To be more definite, let us concentrate on searching for so-called ring-like correlations which are reminiscent of Cherenkov rings, while others will be mentioned only in passing.

Everybody knows about the Cherenkov emission of photons by a bunch of electrons (or of any charged particles, in general) traversing a medium whose refractive index exceeds 1. These photons form a ring in a plane perpendicular to the electrons' motion, i.e. they are emitted at a definite polar angle. As a hadronic analogue, one may treat an impinging nucleus as a bunch of confined quarks (color charges) each of which can emit gluons when traversing a target nucleus. Let me recall that Cherenkov photons are actually a collective effect of emission by the medium which the electrons traverse. In the same spirit, the Cherenkov gluons could result from the collective emission by colliding nuclei. That is why the ring-like structure, if confirmed, would indicate collective long-range correlations in this system.

A long time ago, I speculated [15] about possible Cherenkov gluons relying on the experimental observation of the positive real part of the elastic-forward-scattering amplitude of all hadronic processes at high energies. This is a necessary condition for such a process because in the commonly used formula for the refractive index $n$ its excess over 1 is proportional to this real part:

$$\Delta n(\omega) = \operatorname{Re} n(\omega) - 1 = \frac{2\pi N}{\omega^2} \operatorname{Re} A(\omega, 0^\circ) \approx \frac{3\mu^3}{8\pi\omega} \sigma(\omega)\rho(\omega)\,, \qquad (1)$$

where $\omega$ is the energy of the emitted quantum, $N$ is the density of the scattering centers which has been estimated for hadrons as $N \approx 3\mu^3/(4\pi)$ with pion mass $\mu$, and $A(\omega, 0^\circ)$ is the forward-elastic-scattering amplitude with $\rho(\omega) = \operatorname{Re} A(\omega, 0^\circ)/\operatorname{Im} A(\omega, 0^\circ)$ normalized according to the optical theorem so that $\operatorname{Im} A(\omega, 0^\circ) = \omega\sigma(\omega)/(4\pi)$. Thus the necessary condition for the Cherenkov gluon radiation $\Delta n(\omega) > 0$ is fulfilled if $\rho(\omega) > 0$. For typical values of $\sigma$, $\rho$ and $\omega$ for hadronic processes one gets $\Delta n(\omega) \ll 1$.

However, later [16] I noticed that for such thin targets as hadrons or nuclei a similar effect can appear due to the small confinement length, thus giving us a new tool for estimating it. The bremsstrahlung, the Cherenkov gluons and the transition radiation in thin targets contribute to the same angular range and thus become indistinguishable. At the same time, the difference between bremsstrahlung and Cherenkov radiation can reveal itself in the increased formation length of bremsstrahlung due to relativistic effects, while for Cherenkov radiation the extent of the medium plays a decisive role. Therefore bremsstrahlung will be increased and inclined to smaller polar angles. Thus, the background to Cherenkov radiation seemingly increases. However, as we shall see, it tends to large polar angles in the center-of-mass system, which favors its observation.

The general formula [17] for the total energy $\mathrm{d}W$ in the solid angle $\mathrm{d}\Omega$ due to emission of vector particles with energies ranging from $\omega$ to $\omega + \mathrm{d}\omega$ by a stepwise charge current $|\mathbf{j}_\mu^\perp|$ traversing a target of thickness $l$ and refractive index $n$ with velocity $v = \beta c$ is

$$\frac{\mathrm{d}W}{\mathrm{d}\Omega\,\mathrm{d}\omega} = \frac{e^2\beta^2}{\pi^2 c} \frac{\sin^2\left[\omega l\,(1 - \beta n\cos\theta)\right]}{(1 - \beta n\cos\theta)^2} \sin^2\theta\,, \qquad (2)$$

where $e$ is the electric charge and $\theta$ is the polar angle of photons emission.

Such a stepwise color current was used in Refs [15, 16] as a model for deconfinement of quarks (color) of impinging hadrons (nuclei) only within the volume of the strong-interaction radius $l \sim \mu^{-1}$. Outside this region, quarks are confined, and there are no color currents. Thus, the phenomenological parameter $l$ describes the range of confining forces in normal static hadrons, which just corresponds to the deconfinement region during the collision and wherefrom this collective effect is observed. The spin and mass properties of quarks and gluons are similar to those for electrons and photons, respectively. Therefore, to proceed from the formula (2) to emission of high energy gluons by quarks deconfined in some limited volume (stepwise color current), one should replace $\alpha$ by $\alpha_S C_F$, where $\alpha_S$ is the QCD running coupling, $C_F = 4/3$ and take into account the smallness of the emission angle in the laboratory system $\theta_{\mathrm{l.s.}}$, of the differences $\Delta n = n - 1$ and $1 - \beta$, as well as of the ratio $\mu/\omega$. Then one gets [15, 16] from (2) the inclusive cross section for this gluon radiation

$$\frac{\omega}{\sigma}\frac{\mathrm{d}^3\sigma}{\mathrm{d}^3 k} = \frac{4\alpha_S C_F \theta_{\mathrm{l.s.}}^2 \sin\left[\omega l\,(\theta_{\mathrm{l.s.}}^2 - 2\Delta n)/4\right]}{\pi^2\omega^2(\theta_{\mathrm{l.s.}}^2 - 2\Delta n)^2}\,. \qquad (3)$$

In the case of electromagnetic radiation in macroscopic targets, the condition $\omega l\Delta n/2 \gg 1$ is fulfilled, and the righthand side becomes the Dirac delta-function with an argument corresponding to the condition for the usual Cherenkov rings of photons. In the hadronic case, the

opposite inequality

$$\frac{\omega l \Delta n}{2} \sim \frac{3\rho(\omega)}{16\pi} \ll 1 \tag{4}$$

(for $\sigma \sim \mu^{-2}$, $l \sim \mu^{-1}$) is valid. Thus, the position and the shape of the ring as defined by (3) is determined by the confinement length $l$ but not so much by $\Delta n$.

Surely, the confinement of hadronic partons leads to additional screening of low-energy gluon radiation which acquires a multipole nature because the initial current (a hadron or a nucleus) is colorless, in contrast to the charged current of an electron bunch. Thus, this gluon radiation should be of an even more collective nature and with a harder spectrum than is usually ascribed to the Cherenkov photon radiation. However, it is hard to take into account this collective behavior in a quantitative way. The damping due to the imaginary part of the amplitude was estimated [16] to be unimportant and given by a factor close to 1

$$\exp\left(-\frac{3\mu^2\sigma l}{8\pi}\right) \approx \exp\left(-\frac{\mu l}{8}\right) \approx 0.9\,, \tag{5}$$

which does not prevent the observation of this effect, if any.

If several gluons are emitted and each of them generates a mini-jet centered at a definite polar angle (or pseudorapidity $\eta = -\ln\tan\theta/2$) without any condition imposed on its azimuthal angle $\varphi$, a ring-like substructure will be observed in the target diagram, i.e., in a plane perpendicular to the collision axis. Therefore, events possessing such substructure with relatively short rapidity correlation lengths and large azimuthal correlation lengths would be important to look for. If the density of mini-jets within the ring is so high that they overlap, then they form a (circular) ridge pattern (or a wall pattern according to Ref. [18]). If the number of emitted gluons is not large, we will see several (or just one) jets (tower structure [18]) correlated in their polar, but not in the azimuthal angle. Formula (3) predicts a quite large polar angle of emission of gluons, and therefore a quite large radius of the ring in the target diagram, which favors its observation:

$$\theta_{\text{l.s.}}^{\max} \geqslant \sqrt{\frac{2\pi}{El}}\,, \tag{6}$$

where $E$ is the collision energy. For the deconfinement length of the order of the extension of nuclear forces $l \sim \mu^{-1}$ it gives the following estimate of the polar angles for the rings in the center-of-mass system for two identical particles:

$$\theta_{\text{c.m.s.}} \sim 70^\circ\ (110^\circ)\,, \tag{7}$$

where the angle in the brackets corresponds to the emission in the backward hemisphere by the other colliding particle. If the radiation length for colliding nuclei is proportional to $A^{1/3}$, then the corresponding radiation angle should behave as $A^{-1/6}$. It can be checked in collisions of nuclei with different atomic weights. In a single event, either one or both of these rings can be formed depending on the probability of such a process.

Surely, for the parton-emitter already moving at some angle to the collision axis this ring will be transformed into an ellipse. Central collisions of nuclei would be preferred for the observation of such effects because of the large number of participating partons though the background increases as well due to ordinary process. If the number of correlated particles within the ring is large enough, this would result in spikes in the pseudorapidity distributions. However, the usual histogram method is not always good for verifying these spikes because it may split a single spike into two bins, thus diminishing its role. However, some hints to such a structure can be found from these histograms.

Namely, such a histogram of a cosmic ray nuclear interaction [19] initiated my approach to this problem. A huge spike on the rapidity plot observed in this event was initially interpreted to result from a single cluster. However, since the number of particles in the spike was very high (56 charged particles contributed to it while the average number is about 10), the target diagram was more carefully studied, and it was found that the particles form a ridge in the target diagram (the polar + azimuthal angles plane). There was also an indication for another, more diluted ring-like structure in the backward hemisphere of the same event. High spikes in the pseudorapidity distributions have been observed in some other cosmic ray data [20–23] and in event-by-event analysis of accelerator data [24, 25]. Especially impressive is the famous event of the NA22 Collaboration [25] of the pion–nucleon interaction with a spike 60 times exceeding the average density in the narrow rapidity window. The particles inside the spike are rather uniformly distributed in azimuthal angles (a ridge structure). However, the multiplicities in the analyzed central nucleus-nucleus events are about 50 times higher than in the accelerator data on hadron–hadron collisions. In this case the huge combinatorial background may dilute the strength of the spikes. Anyway, all these events were just single representatives chosen by eye from samples of other events.

It is usually argued that the analysis of a single event of the central nucleus-nucleus collision at high energies may be statistically reliable due to the large number of particles produced. To classify such events in a more quantitative way, one should have a precise method of local pattern recognition on different scales with the possibility of using an inverse transform. This became possible with the advent of the recently developed methods of wavelet analysis. Wavelet analysis is well suited for this purpose because it clearly resolves the local properties of a pattern on an event-by-event basis.

Another example of collective long-range correlations is provided by the so-called elliptic flow, i.e. the azimuthal asymmetry in individual events. This may be related to a collective classical sling-effect [26] of the rotation of colliding nuclei after peripheral collisions initiated by pressure [27] at some impact parameter at the time of collision. In this case some knowledge can be gained about the equation of state of the hadronic matter studying the shapes of the created squeezed states. Another origin of the effect could be due to some jetty structures because the emission of two jets with high transverse momenta well balanced by energy-momentum conservation laws would result in the azimuthal asymmetry of an individual event. These two theoretical suppositions lead however to different event patterns and can be distinguished in experiment. In passing, let me say that elliptic ('cucumber') flow patterns corresponding to large values of the second Fourier coefficient and a 'three-petal-flower' pattern with a large third coefficient were also observed when scanning some high multiplicity events. These results have not yet been published, and I do not discuss all these effects here, concentrating the discussion on the ring-like events only.

The event-by-event analysis of patterns in experimental and Monte Carlo events becomes especially important for very-high-multiplicity collisions at RHIC and LHC. The homogeneous $4\pi$ acceptance of detectors (such as that of the STAR Collaboration at RHIC) will be crucial for it, not to provide false patterns. I am sure that various patterns will be observed, which will allow classifying all events and their 'anomalous' features. Let me stress here, however, that the background due to the ordinary processes of parton emission and rescattering is huge in nucleus-nucleus collisions. It is not clear if the collective effect described above will be noticeable and separable from more common traditional patterns of radiation by individual quarks and gluons. One can rely only on very specific features manifesting themselves as this effect is recorded and on the first positive experience in this respect. Therefore, the clear separation and recognition of these (low-probability?) patterns as objective dynamical effects require new identification methods insensitive to the smooth background and statistical fluctuations (noise). As one of them, I propose to use wavelet analysis and describe recent developments in this area, briefly reviewing some other proposals first.

## 3. Earlier event-by-event studies

When the target diagrams of individual events are analyzed visually, the human eye has a tendency to observing different kinds of intricate patterns with dense clusters (spikes) and rarefied voids in the available phase space. However, the observed effects are often dominated by statistical fluctuations and look quite subjective. The method of factorial moments was proposed [4] to remove the statistical background in a global analysis. It revealed fractal properties even in an event-by-event approach (see Ref. [1]). The increase of the factorial moments for small bins signals the presence of non-statistical fluctuations. Thus, this method may be used as a tool for the preliminary selection of events with strong dynamical fluctuations. Nevertheless, it somehow averages the information about event patterns. Moreover, the patterns in the target diagrams, as seen by eye, hardly differ sometimes [28] in events with different factorial-moment behavior. Some more sensitive and selective criteria should be used.

The first detailed event-by-event analysis [29, 30] of large statistics data on hadron–hadron interactions (unfortunately, however, for a rather low multiplicity) was performed to look for dense groups of particles well separated (isolated) from other particles in the event. The dense groups could resemble single dense jets or ring-like events. Some lower-threshold values were imposed on the density of the groups and on their rapidity distance from other particles. These groups were quite narrow. The rapidity locations of their centers were determined. It has been found that the centers of these groups tend to be positioned at definite polar angles. The positions of the maxima of the centers distribution are quite close to estimates based on formula (7). This feature favors the above interpretation in terms of Cherenkov gluons. Let us note, however, that the search for such fluctuations in the form of dense clusters is interesting by itself, apart from the theoretical interpretation suggested.

For nucleus-nucleus collisions, the first systematic event-by-event analysis was attempted by the NA49 Collaboration [31]. Unfortunately, it was limited to only studies of the fluctuations in the particle transverse momenta and of the relative production of kaons to pions. No evidence was found for unusual fluctuations in the ratios of kaons to pions and in the fluctuations of the transverse momenta even though the latter were much smaller than in nucleon–nucleon collisions (which can be treated on a qualitative level as a result of intranuclear rescatterings). These conclusions do not tell us anything about patterns in individual events. This is not surprising because this experiment has a limited and inhomogeneous acceptance, and only a fraction of the secondary particles are actually recorded. Moreover, this feature of the detector distorts some event characteristics crucial for pattern recognition, e.g., such as the particle density fluctuation. Therefore, the results are not very useful for our purposes.

Full space coverage is ensured only in the traditional emulsion chamber experiments. Therefore it is worthwhile to attempt an event-by-event analysis of their data. Even though the total number of events is relatively low and the particle identification is limited, such data are remarkable for their high angular resolution, which is important for studies of the particle density fluctuations. A very interesting systematic event-by-event analysis of high-multiplicity Pb-Ag/Br collisions at an energy [1] of 158 GeV detected in the EMU13 emulsion experiment was performed by the KLM Collaboration [28]. The results were compared with three different Monte Carlo models: Fritiof, Venus and a random-type model called SMC. It was noticed that even in the one-dimensional distributions the probability of finding a spike and the sizes of spikes are systematically larger in measured events than in simulated ones. This was shown by plotting the distributions of spike fluctuations. The combinatorial background reduces the strength of the observed signals. On the two-dimensional $\eta-\varphi$ phase space plot a slightly stronger clustering (jettyness) of particles in the measured events was also observed, especially for small size clusters. The size of a cluster (cone) was defined as $R=(\delta\eta^2+\delta\varphi^2)^{1/2}$ and the number of particles in the cone was chosen to be greater than 4. The fraction of particles confined in clusters is quite large. No rapidity and azimuthal angle distributions of the cone centers were presented, unfortunately. Therefore, one cannot decide if this effect is only due to short range correlations or some long range correlations like those discussed above are important as well. The only general conclusion is that the phase space inhomogeneity (jettyness) is stronger in the measured events of nucleus-nucleus collisions than in any Monte Carlo models based on the conventional physics of nucleus-nucleus collisions.

In Ref. [32] the azimuthal substructure of particle distributions in individual central high-energy heavy-ion collisions within dense and diluted groups of particles along the rapidity axis was investigated. The data of the EMU01 Collaboration on O/S-Ag/Au collisions at 200 GeV were used. Some criteria appeared to be rather insensitive and did not show any significant difference from the stochastic averages, with $\gamma$-conversion and the HBT particle interference effect taken into account. However, when the parameter

$$S_2=\sum_i\left(\frac{\Delta\varphi_i}{2\pi}\right)^2, \tag{8}$$

[1] Up to now, the nuclear collisions were studied in the external beams only. Therefore, we imply everywhere the energy per nucleon of the impinging nucleus in the rest system of the target nucleus. The impinging nuclei are shown first in front of the dash, and the target nuclei afterwards. It is clear that collisions of different nuclei at colliders will require other conditional notations.

where $\Delta\varphi$ is the azimuthal difference between two neighboring particles in the group and the summation runs over all particles $i$ in the group, was used, some jet structure was revealed for dilute groups, which was impossible to explain by known effects. This is an indication of the ridge-like structure (not a tower structure!) of analyzed groups within definite rapidity windows. This analysis emphasizes the importance of the choice of criteria sensitive enough to features which may be hidden in particular patterns. In my opinion, even the parameter $S_2$, when used in the 'histogram-like' approach with a fixed scale length in pseudorapidity $\Delta\eta$ (as was done in Ref. [32]), averages the fluctuations in individual events too much. More local characteristics should be used in order to avoid smearing the distinct differences between different patterns.

Dense groups were studied in nucleus-nucleus collisions at lower energies. Their rapidity distributions also showed [33] some peaks similar to those found in Refs [29, 30]. However, the fragmentation processes are so strong here that it is not clear how the fragment products influence this conclusion.

## 4. Wavelets: basic notions

All these results, valuable by themselves, still do not answer the question about the existence of long-range correlations in individual events. To obtain an answer, one should be able to perform the large-scale event-by-event analysis . Such a tool is provided by wavelets. Let us briefly describe basic notions about wavelets (for more detail, see Refs [13, 14]).

Commonly used wavelets form a complete orthonormal system of functions with a finite support and can be obtained from one another by dilations and translations. That is why, by changing the scale (dilations), they can distinguish the local characteristics of a signal on various scales and, by translations, they cover the whole region in which it is studied. The orthogonality of wavelets insures that the information on a definite resolution level (scale) does not interfere with other scale information.

Wavelet analysis is the study of any function by expanding it in a wavelet series (or integrals). Due to the completeness of the system, it also allows for the inverse transformation (synthesis) to be done. This means that the original function or some parts of it containing the investigated correlations may be restored without any loss of information. In the analysis of nonstationary signals or inhomogeneous images (like modern paintings with very sharp figure edges), the locality property of wavelets leads to a substantial advantage over the Fourier transform, which provides only the knowledge of global frequencies (scales) of the object under investigation, because the system of functions used (sine, cosine or complex exponents) is defined over an infinite interval.

Wavelet analysis reveals the *local* properties of any pattern in an individual event on *various* scales and, moreover, removes smooth polynomial trends and emphasizes fluctuation patterns. By choosing the strongest fluctuations, one hopes to get rid of statistical fluctuations and observe those dynamic ones which exceed the statistical component.

The traditional formula for the wavelet transform of a one-dimensional function $f(x)$ is written as

$$W(a,b) = a^{-1/2} \int f(x)\, \psi\left(\frac{x-b}{a}\right) \mathrm{d}x\,, \tag{9}$$

where $\psi$ denotes a wavelet with its argument shifted to $x = b$ (translation) and scaled by $a$ (dilation). For continuous wavelets, both $a$ and $b$ are continuous variables. For discrete wavelets, one usually chooses $a = 2^j$, where $j$ are integer numbers, and replaces $b$ by $2^j k$. As we see, the wavelet coefficients for a one-variable function are functions of two variables instead of one variable, as in case of the Fourier transform. This allows us now to define both the scale (frequency) and its effective location.

The choice of the wavelet depends on the problem studied and is not unique. As an example of continuous wavelets, let us mention the so-called 'Mexican hat' wavelet, which is nothing other than the second derivative of the Gaussian function. Discrete wavelets are obtained as solutions of a definite functional equation and cannot be represented in an analytical form. However, they are suitable for computer calculations (for more detail see Refs [13, 14]).

## 5. Wavelet analysis of high-energy nucleus interactions

The first attempts to use wavelet analysis in multiparticle production trace back to P Carruthers [34–36], who used wavelets for the diagonalization of covariance matrices of some simplified cascade models. Ideas of correlation studies in high multiplicity events with the help of wavelets were put forward [37, 38] and used, in particular, for special correlations typical of the disoriented chiral condensate [39, 40]. The wavelet transform of the pseudorapidity spectra of JACEE events was done in Ref. [37].

As was mentioned above, wavelets are most effective in the analysis of inhomogeneous patterns. That is why I proposed using them for deciphering the phase space inhomogeneity (in particular, in the target diagrams) of very-high-multiplicity events.

At present, only five high-multiplicity events of lead-lead collisions at 158 GeV have been analyzed according to this method [41, 42]. I demonstrate here these central Pb-Pb events with the highest registered multiplicities from 1034 to 1221 charged particles chosen from 150 processed events and used for wavelet decomposition with the aim of studying the patterns inherent to them. The data were taken from the emulsion chamber experiment (with a thin lead target) carried out at CERN by the EMU15 group from the Lebedev Physical Institute.

The target diagrams of secondary particle distributions for these events [42] are shown in Fig. 1, where the radial distance from the center is measured by the polar angle $\theta$, and the azimuthal angle $\varphi$ is measured around the center. I show them here to demonstrate that even if one really notices some inhomogeneities in these diagrams, it is not easy to claim which of them are of dynamic origin and, moreover, the whole pattern is strongly influenced by the trivial high energy effect of density increase at small polar angles. Summation over azimuthal angles yields the pseudorapidity ($\eta = -\log\tan\theta/2$) distributions shown in Fig. 2. Pronounced peaks ($\eta$-spikes) strongly exceeding the expected statistical fluctuations are seen in individual events. This inhomogeneity in pseudorapidity can be either due to a very strong jet, i.e. a large group (tower) of particles close in both polar and azimuthal angles, or due to a ring-like (ridge) structure where several jets with smaller number of particles in each of them have similar polar angle but differ in their azimuthal angles. However, it is still not easy to observe them directly in

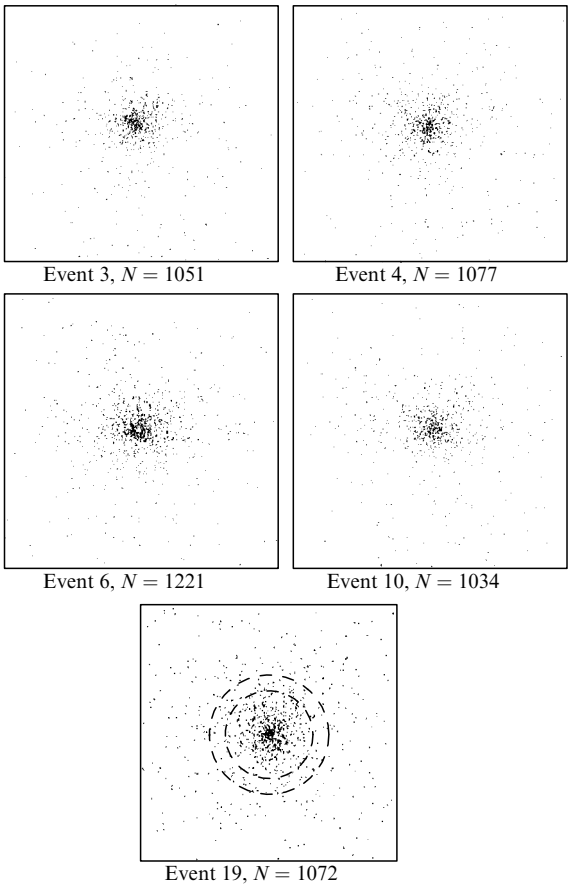


**Figure 1.** Target diagrams of five events of central Pb-Pb collisions at an energy of 158 GeV obtained by the EMU15 collaboration. The radial distance from the center measures the polar angle. The azimuthal angle is counted around the center.

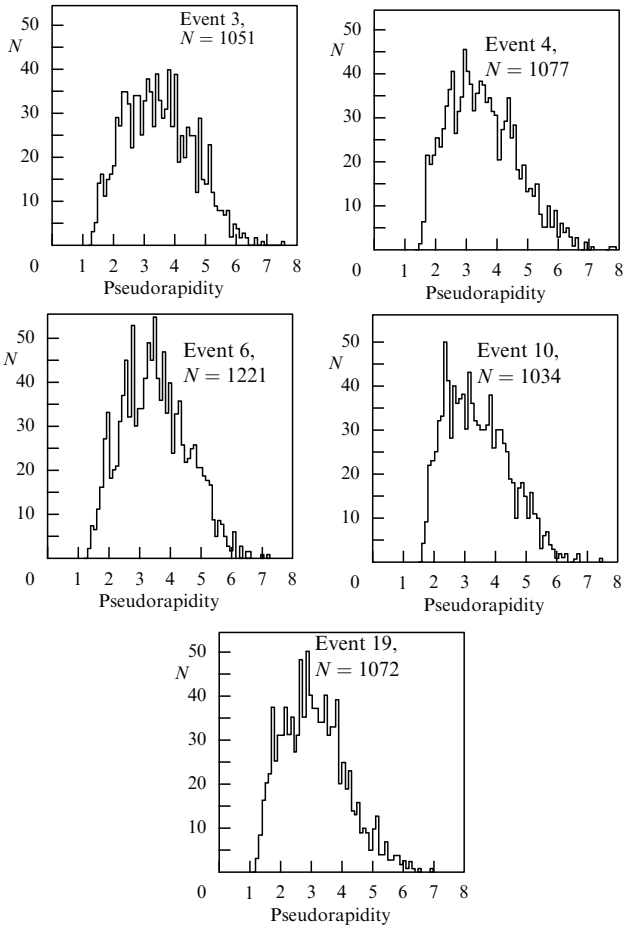


**Figure 2.** Pseudorapidity distributions of particles in the five events of Fig. 1.

the target diagram even if the pseudorapidity is plotted along its radius, instead of the polar angle or the scaled variable [43]

$$\bar{\eta}(\eta) = \int_{\eta_{\min}}^{\eta} \rho(\eta')\,\mathrm{d}\eta' \Big/ \int_{\eta_{\min}}^{\eta_{\max}} \rho(\eta')\,\mathrm{d}\eta' , \qquad (10)$$

which gives rise to a flat distribution $\rho(\bar{\eta})$.

In Ref. [41] wavelets were used for the first time to analyze two-dimensional patterns of fluctuations in the phase space of a single event, shown in Fig. 1 as event 19. The results of the *one-dimensional* analysis of separate sectors of this two-dimensional plot were presented [41]. To proceed in this way, the whole azimuthal region was divided into 24 sectors of $\pi/12$ extent each (thus preserving, unfortunately, the histogram drawback in this coordinate). The pseudorapidity distributions in each of them were separately analyzed after integrating over azimuthal angles within a given sector. Neighboring sectors were connected afterwards.

Both jet and ring-like structures have been found from the values of the squared wavelet coefficients, as seen from Fig. 3, taken from Ref. [41]. Four of the 24 sectors are demonstrated there. The wavelet coefficients were calculated using the continuous 'Mexican hat' wavelet. The darker regions correspond to larger fluctuations, i.e. to larger values of wavelet coefficients. At the very top in each box, i.e. at small scales $a$, the wavelet analysis reveals individual particles as they are placed on the pseudorapidity axis in a given sector; they are seen as short dark lines. At larger scales $a$, corresponding to downward shifts in any box of the figure, correlations of different shapes, corresponding to clusters or jets of particles are resolved. Finally, at even larger scales, one notices a long-range structure (indicated by the arrows in Fig. 3) which penetrates from one azimuthal sector to the neighboring one at nearby values of the polar angle (pseudorapidity), thus forming an elliptic ridge around the center of the target diagram. This structure approximately corresponds to the peak in the pseudorapidity distribution (for more detail, see Ref. [41]). Let us note that it is not easy to notice by eye in the target diagram of this event, shown in Fig. 1, any increase of density at the ring, because of the specific properties of the $\theta-\varphi$ plot, where the density of particles decreases fast toward the external region of large polar angles, due to relativistic effects. Also, the tree-like patterns in this plot of the wavelet coefficients probably correspond to the fractal structure of the phase space, which was discovered by the factorial moments method.

To study these patterns in more detail, one should perform a *two-dimensional* local analysis. It is strongly desirable to get rid of the drawback of the histogram method: the fixed positions of the bins sometimes give rise to the splitting of a jet into pieces contained in two or more bins, as, e.g., it could happen in the above analysis of the event 19 [41] when 24 azimuthal sectors were chosen. Moreover, the number of charged particles in each sector was about 50, which is already at the limits of the accuracy for efficient wavelet analysis. The two-dimensional wavelet transform of

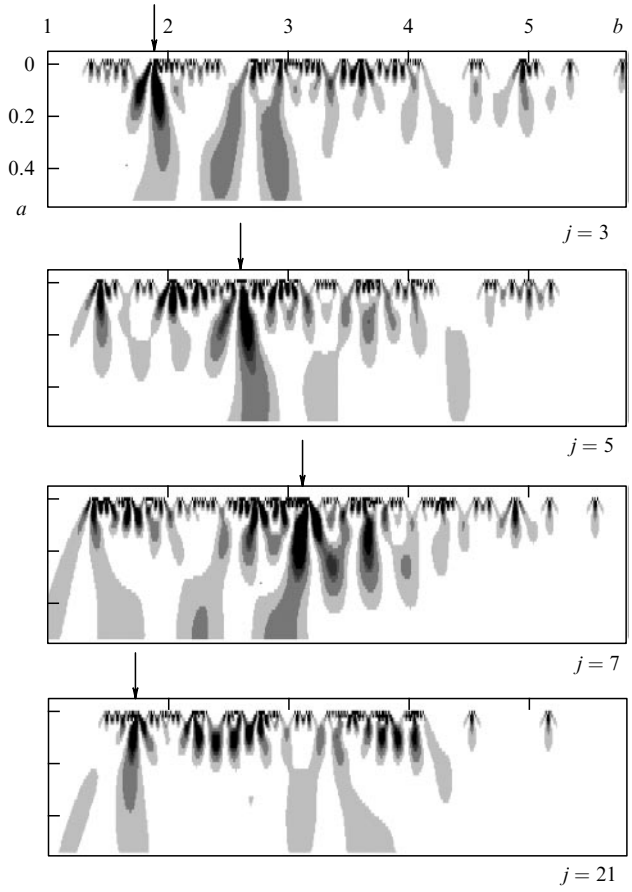


**Figure 3.** Wavelet coefficients for event 19 analyzed in Ref. [41]. Dark regions correspond to large values of the coefficients. Four of 24 sectors are shown. The rapidities are along the $x$-axis; the scales increase down the vertical axis.

particle densities obtained directly in the two-dimensional plot does not have such a deficiency. Wavelets automatically choose the sizes and shapes of bins (so-called Heisenberg windows; see, e.g., Ref. [11]), depending on the particle density at a given position. The bin becomes small if the changes (fluctuations) are abrupt, and large if the function varies slowly. Multiresolution analysis at different scales and in different regions is performed.

In principle, the wavelet coefficients $W_{j_1,k_1,j_2,k_2}$ of the two-dimensional function $f(\theta,\varphi)$ are found from the formula

$$W_{j_1,k_1,j_2,k_2} = \int f(\theta,\varphi)\psi(2^{-j_1}\theta - k_1; 2^{-j_2}\varphi - k_2)\,\mathrm{d}\theta\,\mathrm{d}\varphi\,. \quad (11)$$

Here $\theta_i$, $\varphi_i$ are the polar and azimuthal angles of the particles produced,

$$f(\theta,\varphi) = \sum_i \delta(\theta - \theta_i)\delta(\varphi - \varphi_i)\,,$$

with the summation over all particles $i$ in a given event, $(k_1,k_2)$ denoting the locations and $(j_1,j_2)$, the scales analyzed. The function $\psi$ is the analyzing wavelet. The higher the density fluctuations of particles in a given region, the larger are the corresponding wavelet coefficients.

In practice, the discrete wavelets obtained as the tensor product of two multiresolution representations of standard one-dimensional Daubechies 8-tap wavelets were used. Then the corresponding *ss*, *sd* and *dd* coefficients in the two-dimensional matrix were calculated (see Ref. [11]). The common scale $j_1 = j_2 = j$ was used. This simplifies the calculations and the representation of the obtained results because of the smaller number of variables but may not be completely satisfactory from the physical point of view and, probably, should be abandoned later in a more sophisticated approach. A similar basis was used in Ref. [44].

As stressed above, the ring-like structure should be a collective effect involving many particles and large scales. Therefore, to get rid of the low-scale background due to individual particles and analyze their clusterization properties, the scales $j > 5$ were chosen, on which both single jets and those clustered in ring-like structures can be revealed, as seen from Fig. 3. Therefore, all coefficients with $j < 6$ were put equal to 0. The wavelet coefficients for any $j$ from the interval $6 \leqslant j \leqslant 10$ were represented as functions of polar and azimuthal angles in the form of a two-dimensional landscape-like surface over this plane, i.e. over the target diagram. Their inverse wavelet transform allows modified target diagrams of analyzed events, with only large-scale structures left, to be obtained. Higher fluctuations of particle density inside large-scale formations and, consequently, larger wavelet coefficients correspond to darker regions in this modified target diagram shown in Fig. 4. Here we demonstrate two events (3 and 6) from the five ones shown in Figs 1 and 2. They clearly display both jet and ring-like structures, which are different in different events. To discard the methodical cut-off at $\eta \approx 1.6-1.8$, only the region of $\eta > 1.8$ was considered [2].

Even though the statistics are very low, it was attempted to plot the pseudorapidity distribution of the maxima of the wavelet coefficients with the hope to see if it reveals the peculiarities observed in high statistics but low multiplicity hadron-hadron experiments [29, 30]. In Fig. 5, the number of highest maxima of the wavelet coefficients exceeding the threshold value $W_{j,k} > 2 \times 10^{-3}$ is plotted as a function of their pseudorapidity for all five events considered. It is quite peculiar that the positions of the maxima are discrete. They are positioned quite symmetrically about the value $\eta \approx 2.9$ corresponding to 90° in the center-of-mass system as should be for two Pb nuclei colliding. The difference of heights is within the error bars. More interestingly, they do not fill in this central region but are rather separated. Qualitatively, this coincides with the findings in Refs [29, 30], where the separated peaks in the pseudorapidity distribution of the centers of dense groups were also noticed approximately at the same positions.

For comparison, 100 central Pb-Pb interactions were generated with energy 158 GeV according to the Fritiof model and the same number of events, according to the random model describing the inclusive rapidity distribution shape. The fluctuations in these simulated high multiplicity events are much smaller than in experimental ones and do not show any ring-like structure.

Further wavelet analyses based on different scales for polar and azimuthal angles and studies of the 3-dimensional phase space are desirable. For the latter, one needs data on the momenta of the created particles, which may be obtained only in experiments with a magnetic field. Though the emulsion chamber of the EMU15 experiment was installed in a

[2] A more detailed discussion of this methodical effect can be found in Ref. [42]. It shows that wavelets may be used for the analysis of methodical problems in detectors as well. This topic is out of the scope of the present paper.

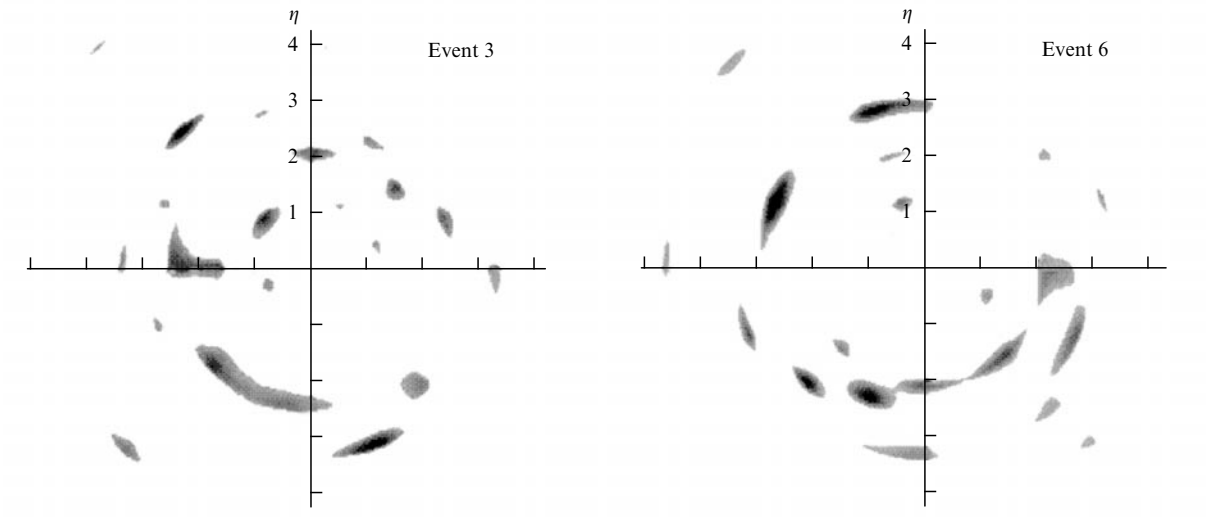


**Figure 4.** Modified large-scale target diagrams of two events (3 and 6). Darker regions correspond to larger particle density fluctuations.

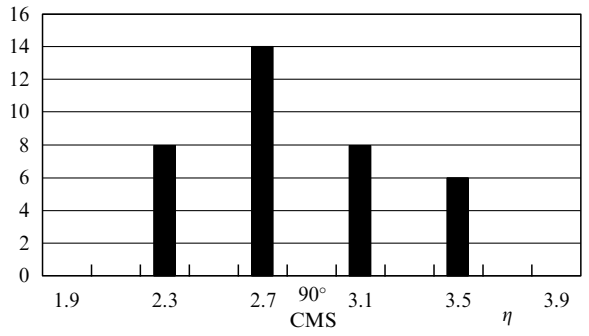


**Figure 5.** Pseudorapidity distribution of the maxima of wavelet coefficients. The irregularity in the maxima positions, the empty voids between them and the absence of peaks at $\eta \approx 2.9$ are noted. The pseudorapidity is plotted on the $x$-axis; the number of maxima, on $y$-axis.

magnetic field $H = 1.8$ T, no measurements of the trajectory curvature have been made until now. Thus, data on the three-dimensional phase space are not yet available. I would like to stress once more that a good homogeneous acceptance of the detectors with a $4\pi$ geometry is crucial for the proper wavelet analysis of any event to get firm conclusions about the dynamic effects. Otherwise the results will show an admixture of physical and methodical effects which cannot be distinguished by an event-by-event analysis. Actually, this remark is a byproduct of my own experience in attempts to find the elliptic flow effect in the NA49 data on lead-lead collisions at 158 GeV. These attempts failed because, although I noticed an azimuthal asymmetry to persist at the same position, I also suspected it to be due to the inhomogeneous azimuthal acceptance of the detector, and after enquiring was assured by the authors that my guess was correct. Thus, the methodical effect was so strong that it prevented any conclusions about the dynamic elliptic flow but, probably, would not prevent the analysis of some structures in polar angles to be done. Even though such applications of the wavelet analysis are interesting by themselves and their effectiveness was demonstrated in this case, they are not of the main physics interest and of concern here.

## 6. Conclusions

Thus, I conclude that, even on the qualitative level, there is a noticeable difference between experimental and simulated events, with larger and somewhat ordered fluctuations in the former. The first attempts to apply the method of wavelet analysis described here have shown some peculiar patterns of individual measured events not resolved in the Monte Carlo simulated samples. This means that we still have something to learn about their dynamic features. The ring-like patterns were used here only as an example of possible correlations leading to some special particle grouping in the phase space. More detailed wavelet analyses at various resolution levels and also in the three dimensional phase space may reveal some yet undiscovered structures. The efforts described above show that there are no unsolvable problems in doing it.

My aim here was to show the applicability and power of the new method of two-dimensional wavelet analysis and its qualitative features and differences, leaving aside quantitative characteristics until higher statistics of AA-events with a reliably documented high multiplicity become available. In particular, a special automatic complex for emulsion processing with a high space (angular) resolution (www.lebedev.ru/structure/pavicom/index.htm) is coming into operation at the Lebedev Physical Institute, and it can make it possible to enlarge the statistics of analyzed central Pb-Pb collisions at 158 GeV quite soon, using at full strength the good acceptance and precision of emulsion detectors. Also the data of the STAR collaboration in RHIC with a full phase space coverage and a large number of events should soon be available at even higher energies. Wavelets provide a powerful tool for event-by-event analysis of fluctuation patterns in such collisions.

## References

1. De Wolf E A, Dremin I M, Kittel W *Phys. Rep.* **270** 1 (1996)
2. Khoze V A, Ochs W *Int. J. Mod. Phys. A* **12** 2949 (1997)
3. Dremin I M, Gary J W *Phys. Rep.* (2001) (to be published); hep-ph/0004215
4. Bialas A, Peschanski R *Nucl. Phys. B* **273** 703 (1986)
5. Dremin I M, in *Festschrift to L. Van Hove* (Eds A Giovannini, W Kittel) (Singapore: World Scientific, 1990) p. 455
6. Ochs W, Wosiek J *Phys. Lett. B* **289** 159 (1992); **305** 144 (1993)

7. Dokshitzer Yu L, Dremin I M *Nucl. Phys. B* **402** 139 (1993)
8. Brax P, Meunier J-L, Peschanski R *Z. Phys. C* **62** 649 (1994)
9. Dremin I M *Phys. Lett. B* **313** 209 (1993)
10. Dremin I M, Nechitailo V A *Mod. Phys. Lett. A* **9** 1471 (1994)
11. Daubechies I *Ten Lectures on Wavelets* (CBMS-NSF Regional Conf. Ser. in Applied Math., 61) (Philadelphia, Pa.: SIAM, 1992)
12. Meyer Y *Wavelets*: *Algorithms & Applications* (Philadelphia, Pa.: SIAM, 1993)
13. Astaf'eva N M *Usp. Fiz. Nauk* **166** 1145 (1996) [*Phys. Usp.* **39** 1085 (1996)]
14. Dremin I M, Ivanov O V, Nechitaĭlo V A *Usp. Fiz. Nauk* (2001) (to be published)
15. Dremin I M *Pis'ma Zh. Eksp. Teor. Fiz.* **30** 152 (1979) [*JETP Lett.* **30** 140 (1979)]; **34** 617 (1981) [*JETP Lett.* **34** 594 (1981)]
16. Dremin I M *Yad. Fiz.* **33** 1357 (1981) [*Sov. J. Nucl. Phys.* **33** 726 (1981)]
17. Frank I M, Tamm I E *Dokl. Akad. Nauk SSSR* **14** 107 (1937); *J. Phys. USSR* **1** 439 (1939)
18. Peschanski R, in *Proc. XXII Intern. Symp. on Multiparticle Dynamics, Santiago de Compostela, Spain, 1992* (Ed. C Pajares) (Singapore: World Scientific, 1993) p. 241
19. Apanasenko A V et al. *Pis'ma Zh. Eksp. Teor. Fiz.* **30** 157 (1979) [*JETP Lett.* **30** 145 (1979)]
20. Alekseeva K I et al. *Izv. Akad. Nauk SSSR Ser. Fiz.* **26** 572 (1962); *J. Phys. Soc. Jpn. Suppl. A-III* **17** 409 (1962)
21. Maslennikova N V et al. *Izv. Akad. Nauk SSSR Ser. Fiz.* **36** 1696 (1972)
22. Arata N *Nuovo Cimento A* **43** 455 (1978)
23. Dremin I M, Orlov A M, Tret'yakova M I *Pis'ma Zh. Eksp. Teor. Fiz.* **40** 320 (1984) [*JETP Lett.* **40** 1115 (1984)]; *Proc. 17th ICRC* **5** 149 (1981)
24. Marutyan N A et al. *Yad. Fiz.* **29** 1566 (1979) [*Sov. J. Nucl. Phys.* **29** 804 (1979)]
25. Adamus M et al. (NA22 Collab.) *Phys. Lett. B* **185** 200 (1987)
26. Dremin I M, Man'ko V I *Nuovo Cimento A* **111** 439 (1998)
27. Ollitrault J-Y *Phys. Rev. D* **46** 229 (1992); **48** 1132 (1993)
28. Cherry M L et al. (KLM Collab.) *Acta Phys. Pol. B* **29** 2129 (1998)
29. Dremin I M et al. *Yad. Fiz.* **52** 840 (1990) [*Sov. J. Nucl. Phys.* **52** 536 (1990)]; *Mod. Phys. Lett. A* **5** 1743 (1990)
30. Agababyan N M et al. (NA22 Collab.) *Phys. Lett. B* **389** 397 (1996)
31. Roland G (NA49 Collab.) *Nucl. Phys. A* **638** 91c (1998)
32. Adamovich M I et al. (EMU01 Collab.) *J. Phys. G* **19** 2035 (1993)
33. Gogiberidze G L, Gelovani L K, Sarkisian E K *Phys. Lett. B* **471** 257 (1999)
34. Carruthers P, in *Proc. of a NATO Adv. Study Inst. on Hot and Dense Nuclear Matter, Bodrum, Turkey, 1993* (NATO ASI Series, Ser. B, Vol. 335, Eds W Greiner, H Stücker, A Gallmann) (New York: Plenum Press, 1994) p. 65
35. Lipa P, Greiner M, Carruthers P, in *Proc. of the Cracow Workshop on Multiparticle Product. Soft Physics and Fluctuations, Cracow, Poland, 1993* (Eds A Bialas et al.) (Singapore: World Scientific, 1994) p. 105
36. Greiner M et al. *Z. Phys. C* **69** 305 (1996)
37. Suzuki N, Biyajima M, Ohsawa A *Prog. Theor. Phys.* **94** 91 (1995)
38. Huang D *Phys. Rev. D* **56** 3961 (1997)
39. Zheng Huang et al. *Phys. Rev. D* **54** 750 (1996)
40. Nandi B K et al. (WA98 Collab.), in *Proc. of the 3rd Intern. Conf. on Physics and Astrophysics of Quark-Gluon Plasma, Jaipur, India, 1997* (Eds B C Sinha, D K Srivastava, Y P Viyogi) (New Delhi: Narosa Publ. House, 1998) p. 12
41. Astafyeva N M, Dremin I M, Kotelnikov K A *Mod. Phys. Lett. A* **12** 1185 (1997)
42. Dremin I M et al. *Phys. Lett. B* (2000) (to be published); hep-ph/0007060
43. Bialas A, Gazdzicki M *Phys. Lett. B* **252** 483 (1990)
44. Goedecker S, Ivanov O V *Comp. Phys.* **12** 548 (1998)